Rolling contact fatigue performance of a TiN coating deposited on AISI 440C by plasma based ion implantion and deposition

María Paula González, Diego A. Colombo, Diego O. Fernandino
Instituto de Investigaciones en Ciencia y Tecnología de los Materiales, Universidad Nacional de Mar del Plata, Facultad de Ingeniería, CONICET, Argentina.
mpgonzalez@fi.mdp.edu.ar, diegocolombo@fi.mdp.edu.ar, dfernandino@fi.mdp.edu.ar

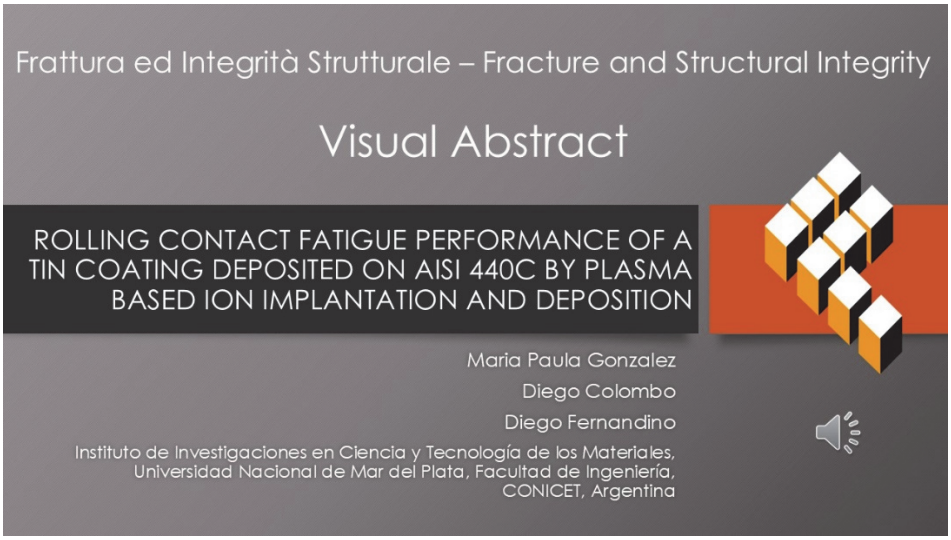

Citation: Gonzalez, M.P., Colombo, D.A., Fernandino, D.O., Rolling contact fatigue of AISI 440C TiN coated by plasma based ion implantation and deposition, Frattura ed Integrità Strutturale, 72 (2025) 15-25.

Received: 06.11.2024
Accepted: 12.12.2024
Published: 07.01.2025
Issue: 04.2025

KEYWORDS. AISI 440C, PBII&D, TiN, wear, rolling contact fatigue.

INTRODUCTION

Martensitic stainless steels are widely recognized as engineering materials due to their exceptional hardness, mechanical strength, and wear resistance, even with moderate corrosion resistance. These alloys, primarily composed of Fe-Cr-C, can be categorized based on their carbon content into low, medium, and high. Notably, AISI 440C, a high carbon martensitic stainless steel, demonstrates superior mechanical properties relative to its counterparts. The high carbon content in AISI 440C makes its mechanical strength and corrosion resistance highly sensitive to heat treatment processes. Typically, the steel is initially treated in an annealed state before undergoing hardening through solid-state phase transformations. This steel is often utilized in the production of mechanical components that demand a hardness level of approximately 60 HRC (with a tempering temperature around 200 °C), particularly in applications involving rolling or sliding contacts, such as roller bearings and seaming rolls. A significant failure mode for these components is rolling contact fatigue (RCF), a wear mechanism driven by material removal under cyclic loading conditions [1].
Furthermore, it is well established that the performance of components under wear and/or corrosion is closely linked to the surface properties and characteristics, which can be enhanced through various surface treatment techniques [2]. Among

these treatments, hard coatings applied via physical vapor deposition (PVD) methods have proven effective in enhancing the corrosion and wear resistance of a diverse range of metal substrates [3-5]. Research indicates that the optimal coating thickness for RCF performance is approximately 0.75 μm [6]. Additionally, achieving a relatively high deposition temperature (above 300°C) is crucial for producing dense and well-adhered PVD coatings [7]; however, this may lead to microstructural degradation in heat-treated substrates.

There is a notable lack of literature addressing the RCF behavior of AISI 440C, AISI 52100, and other high hardness steels treated with PVD coatings. Moreover, only a limited number of studies have examined how deposition temperature influences the microstructural evolution of these substrates [8, 9]. Findings suggest that if the hardness of the substrate decreases by more than 2 HRC, the effectiveness of the coatings in RCF applications diminishes. This is attributed to an increasing mismatch in properties between substrate and coating as substrate hardness declines. Additionally, softening of the substrate can negatively affect the performance of components in service. Consequently, the choice of deposition temperature emerges as a critical consideration when selecting a coating process for high hardness steels.

The concept of functionally graded materials (FGMs) offers a potential solution to mitigate the abrupt property transitions between substrate and coating [10]. FGMs are advanced composites characterized by a gradual variation in structure and/or composition, enabling the design of tailored morphologies and mechanical properties. Compositional gradient nitride coatings can be effectively deposited through PVD by manipulating bias voltage or nitrogen flow [11,12]. Another promising technique, plasma-based ion implantation and deposition (PBII&D), can further minimize property mismatches. This combined method involves inserting a sample into plasma and applying high-voltage pulses, resulting in ion implantation during pulse activation. This approach facilitates the formation of a mixing zone at the substrate/coating interface, preventing abrupt property changes, as high-energy impacts implant atoms beneath the substrate surface [13]. Unlike conventional PVD processes, PBII&D can be conducted at room temperature without sacrificing coating adhesion, thereby preserving the integrity of hardened substrates.

To the best of the author's knowledge, there are no references about the deposition of functionally gradient coatings on martensitic stainless steels to improve their surface properties and wear resistance. On this basis, the aim of this work is to study the microstructural evolution, surface characteristics and RCF behavior of high hardness AISI 440C samples (about 60 HRC) coated with a TiN film synthesized by PBII&D at room temperature.

EXPERIMENTAL PROCEDURES

Substrate material and sample preparation

In this study, solid bars of AISI 440C steel were used, each with a diameter of 70 mm and a length of 100 mm. The chemical composition, analyzed through optical emission spectrometry, was as follows (in wt%): C=1, Cr=18.5, Ni=0.1, Mo=0.5, Si=0.4, P=0.03, S=0.01, Mn=0.3, W=0.04, with iron as the balance.

The bars were subsequently cut and machined by turning to fabricate disc samples with a diameter of 60 mm and a thickness of approximately 8 mm. The heat treatment process comprised three main stages: an initial austenitizing at 1000 °C for 180 minutes, followed by oil quenching, and finally a tempering stage conducted in a salt bath at 200 °C.

For the finishing process, conventional straight surface grinding was employed. This involved the use of a peripheral surface grinder with a horizontal spindle and a reciprocating table, conducting three roughing passes and a single finishing pass on each sample. The objective of the finishing pass was to achieve a low surface roughness. A vitrified grinding wheel containing SiC abrasive grains was used, while an oil-in-water emulsion (Dromus B at 5%) served as the coolant. Additionally, control samples intended for instrumented indentation tests were polished using water-based SiC sandpaper up to a grit size of 1000, and subsequently finished to a mirror-like finish using a damp cloth with alumina.

Coating process

The coatings were produced using an experimental direct current (DC) cathodic arc deposition system. Prior to loading the samples into the vacuum chamber, they underwent thorough cleaning involving ultrasonic baths with industrial degreaser, acetone, and alcohol, each for 10 minutes. After drying, the samples were placed in the chamber and evacuated to establish a base pressure, followed by an argon glow discharge lasting 60 minutes to ensure surface cleanliness.

The substrate holder was positioned 200 mm from the front surface of the cathode. Importantly, all depositions were conducted at room temperature, without the use of external heating. Consequently, the process parameters were specifically optimized for this condition.

The optimal deposition parameters were identified as a discharge current of 100 A, negative pulses with a peak voltage of 6 kV (operating at a frequency of 200 Hz with a pulse width of 50 μs), and a nitrogen flow rate of 22 sccm to maintain a discharge pressure of 4 x 10^{-4} mbar. An initial discharge lasting 2 minutes was performed without nitrogen, leading to the formation of a pure titanium adhesion interlayer. This was followed by the deposition of the TiN coating for a duration of 10 minutes. The parameters used in this process are summarized in Tab. 1, highlighting that deposition times were carefully adjusted to achieve a final film thickness of approximately 0.75 μm.

Layer	Distance anode-cathode (mm)	Arc current (A)	Polarization			Pressure (mbar)	Flow N_2 (sccm)	Time (minutes)
			Voltage (kV)	Frequency (Hz)	Pulse width (μs)			
Ti	200	100	-6	200	50	$1x10^{-5}$	-	2
TiN						$4x10^{-4}$	22	10

Table 1: Deposition parameters of PBII&D process.

Substrate and coating characterization

The microstructure of AISI 440C was analyzed both before and after the application of coatings using optical microscopy. Metallographic etching to reveal microstructural details was conducted with Vilella. For phase identification, X-ray diffraction (XRD) was employed, utilizing a Panalytical Empyrean diffractometer with a PIXCEL 3D detector. The XRD patterns were recorded over a 2θ range of 30° to 90°. To evaluate the hardness of the AISI 440C substrates, both prior to and following coating deposition, a conventional hardness tester was used to measure Rockwell-C hardness.

The roughness profiles of the uncoated and coated samples were characterized by assessing the conventional arithmetic average height (Ra) and skewness (Rsk) using a stylus profilometer (Taylor-Holson Surtonic +3) with a cut-off of 0.8 mm and a 4 mm evaluation length. Hardness (H_{IT}) and reduced elastic modulus measurements for the substrate phases in uncoated samples, as well as for the coating in coated samples, were performed using a Hysitron TI 900 Triboindenter. Coating thickness was determined by the Calotest method, which involved the use of a 25.4 mm diameter bearing ball along with diamond polishing paste of ¼ μm granularity. Adhesion of the coatings was evaluated through the Rockwell-C adhesion test in accordance with the VDI 3198 standard [14].

Rolling contact fatigue test

The RCF tests were executed using a flat washer-type testing apparatus, designed to operate under lubricated pure rolling conditions. A schematic illustration of this testing setup is provided in Fig. 1. For these experiments, a standard 52106 thrust ball bearing with six balls mounted in the cage was utilized as the counterpart. The rotational speed of the samples was maintained at 1650 rpm, translating to a loading frequency of approximately $2.97x10^5$ cycles/hour. For lubrication, a commercial hydraulic oil with a kinematic viscosity of 100 cSt at 40 °C was employed. The tests were conducted under a maximum contact pressure (p_0) of 3.7 GPa. The specific oil film thickness (λ) was observed to vary between 0.75 for coated samples and 0.98 for uncoated samples, establishing a boundary lubrication regime [15]. This regime may lead to increased direct contact between surface irregularities of the contacting bodies. As a result, the coated samples exhibit a heightened susceptibility to surface crack initiation, attributed to their lower λ value.

A total of ten RCF tests were conducted on both uncoated and coated samples. Each specimen was subjected to test conditions until a noticeable macroscopic fatigue failure was observed or until a maximum of 500 hours of operation was reached without any failures. The failure times for the samples were recorded using a timer, which were then converted into loading cycles for analysis. To evaluate the rolling tracks of the samples, profilometry, scanning electron microscopy (SEM), and energy-dispersive X-ray spectroscopy (EDS) were employed.

The results of the RCF tests were analyzed using a two-parameter Weibull distribution. Although suspensions are not illustrated in the Weibull plots, they were included in the overall analysis. Life data fitting was conducted using rank regression methods [16]. To facilitate comparisons, the estimated lifetimes for 10% (L10) and 50% (L50) probabilities of failure were calculated. Additionally, two-sided 90% confidence intervals for each sample set were determined through pivotal functions using Monte Carlo simulations [17]. The entire statistical analysis was performed with the aid of the free software R.

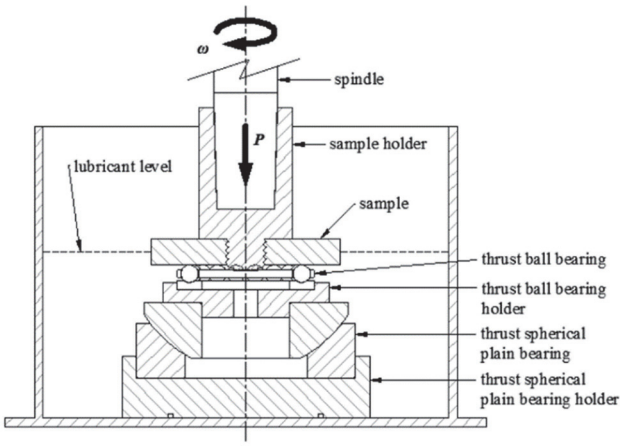

Figure 1: Schematic view of the RCF testing rig.

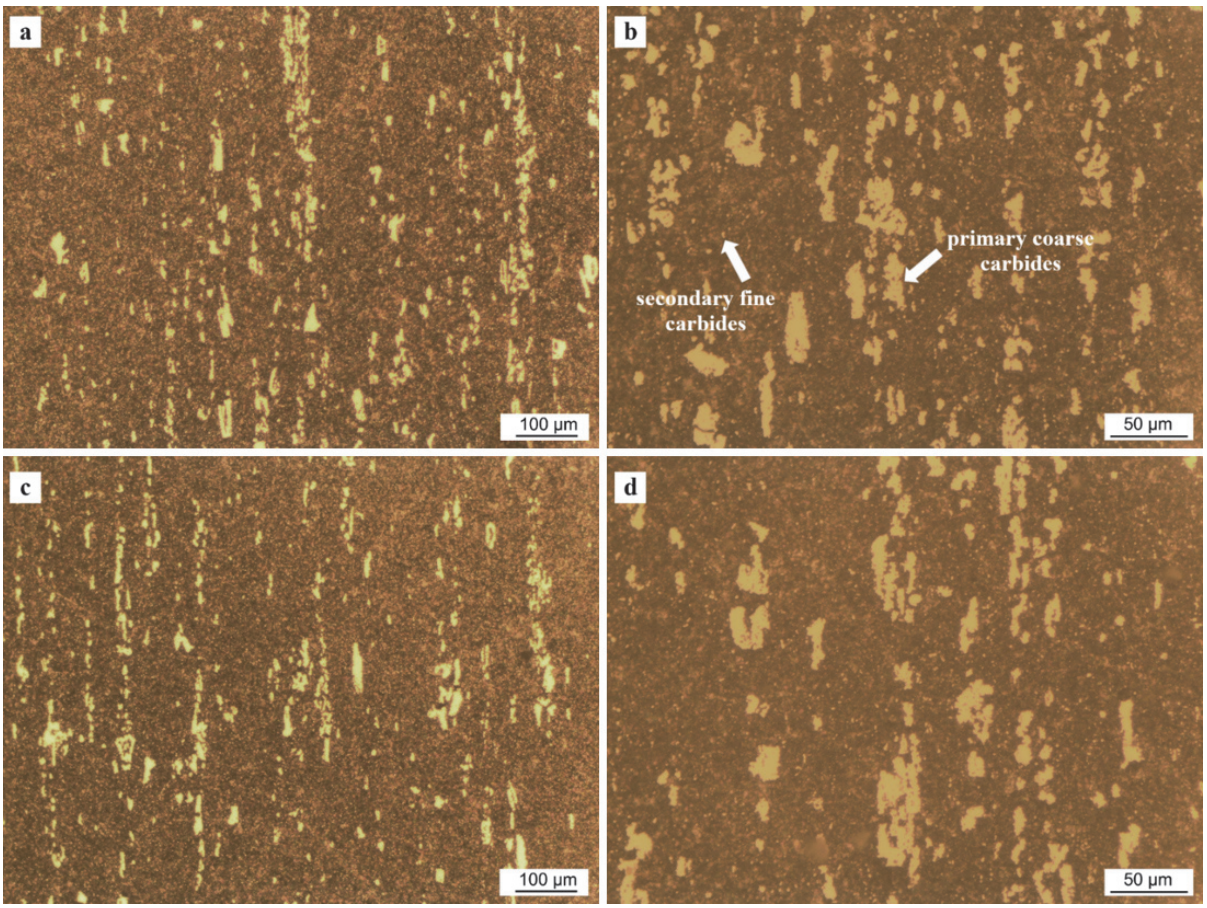

Figure 2: Microstructure of AISI 440C. a) before deposition 200x, b) before deposition 500x, c) after deposition 200x, d) after deposition 500x.

RESULTS AND DISCUSSION

Substrate and coating characteristics

Fig. 2 contrasts the microstructure of AISI 440C before and after coating deposition. The resulting microstructure of AISI 440C after quenching and tempering is shown in Figs. 2a and 2b. It is composed of a martensitic matrix of very fine needles and carbides dispersed in the matrix. Two families of carbides can be noted, one with irregular geometry and sizes in the range of 5 µm to 25 µm approximately (primary coarse M_7C_3 carbides) and another with a more

regular geometry and sizes in the order of 1 μm or less (secondary fine $M_{23}C_6$ carbides). Primary carbides precipitate directly from the liquid in interdendritic regions, while secondary carbides are formed during solid-state reactions [18]. It is also observed that the primary carbides form bands in the microstructure of the steel (Fig. 2a), while the secondary carbides are more randomly distributed (Fig. 2b). In Figs. 2c and 2d the microstructure of the coated substrates is analogous to that of the uncoated ones. In addition, the hardness of the substrates was maintained between 59 HRC and 60 HRC before and after deposition. Therefore, it can be said that the coating process does not produce a microstructural change of the substrates and that can be applied to materials whose thermal treatment involves low tempering temperatures.

The XRD diffraction patterns of coated and uncoated samples are shown in Fig. 3. Fig. 3a reveals the main diffraction packs of martensite (α') and the carbides (*). The overlapping of orientations of the martensite phase can be observed. This is because the tetragonality of sample is very low. In addition, the presence of retained austenite (γ) in the microstructure of steel can be noted, due to the martensite finish temperature (Mf) is below room temperature. Fig. 3b reveals the main diffraction packs of TiN together with some substrate peaks, due to the penetration depth of the X-rays is greater than the coating thickness. The diffractogram indicates that the TiN coating grew with a NaCl-type cubic structure and without a clearly defined preferential orientation.

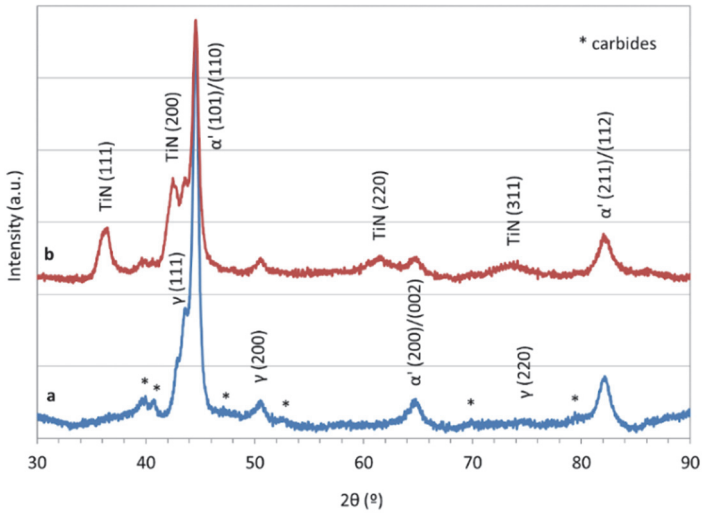

Figure 3: XRD patterns of uncoated and coated samples. a) AISI 440C. b) AISI 440C - TiN.

The surface characteristics of the uncoated and coated samples, such as coating thickness, arithmetic average height and skewness of the roughness profiles, hardness and elastic modulus of substrate phases and coating, are listed in Tab. 2. The Ra and Rsk values obtained for the AISI 440C samples after the grinding operations were 0.233 μm and -0.025 μm, respectively. The almost zero Rsk value indicate that profiles are quite symmetrical with respect to the mean line, that is, they have no preponderance of very high peaks or very deep valleys. Regarding AISI 440C hardness and elastic modulus, it can be noted that the hardness of the primary carbides is approximately twice that of the metal matrix, with average values of 20.67 GPa and 10.63 GPa, respectively. These values obtained are consistent with bibliographic data [18]. The reduced elastic modulus of the primary carbides (211.75 GPa) is also higher than that of the metal matrix (196.57 GPa), although the difference is less significant.

The average thickness obtained for the TiN coating deposited on the AISI 440C specimens was 0.84 μm. The Ra and Rsk values of the coated samples were 0.304 μm and 0.143 μm, respectively. The higher Ra and the positive skewness of the coated samples, when compared to the uncoated AISI 440 C, can be ascribed to the presence of macroparticles within the coating [19]. This phenomenon is due to the fact that the evaporation of the target material in a cathodic arc system is always accompanied by the release of small amounts of liquid particles (also referred to as macroparticles) that are incorporated into the plasma as droplets, transported towards the substrate surface and attached to the film, modifying its topography. Fig. 4 shows the presence of macroparticles adhered to the film. The average values of hardness and elastic modulus obtained for the TiN coating were 30.93 and 256.81 GPa, respectively. The values obtained are consistent with those reported in the literature for the same deposition process [20, 21]. If these results are compared with those of the uncoated samples, it can be noted that the hardness of the TiN coating is 3 times that of the metallic matrix and 1.5 times that of the primary carbides. The reduced elastic modulus of the coating is also higher than those of the matrix and the primary carbides, but the differences are relatively slight.

Sample		Film thickness (μm)	Ra (μm)	Rsk	H_{IT}(GPa)	Er (GPa)
AISI 440C	Metal matrix	--	0.233±0.004	-0.025±0.049	10.63±0.58	196.57±3.90
	Primary carbides				20.67±1.12	211.75±5.96
AISI 440C-TiN		0.84±0.04	0.304±0.014	0.143±0.099	30.93±2.11	256.81±11.72

Table 2: Properties of the uncoated and coated samples.

The adhesion strength quality of the TiN coatings to the AISI 440C substrates, as determined by the Rockwell–C adhesion test, can be classified as HF1. No delamination was observed in any case. Fig. 5 shows, as an example, an imprint generated by the adhesion test. This adhesion strength was commonly observed in PVD coatings deposited at temperatures above 300 °C [20, 22]. However, due to the mixing zone formed by the PBII&D process at the substrate/coating interface, a very good adhesion strength can also be obtained at room temperature.

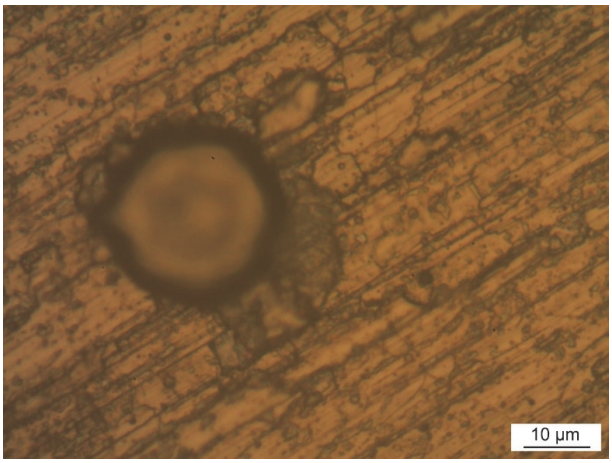

Figure 4: Macroparticle attached to the TiN coating.

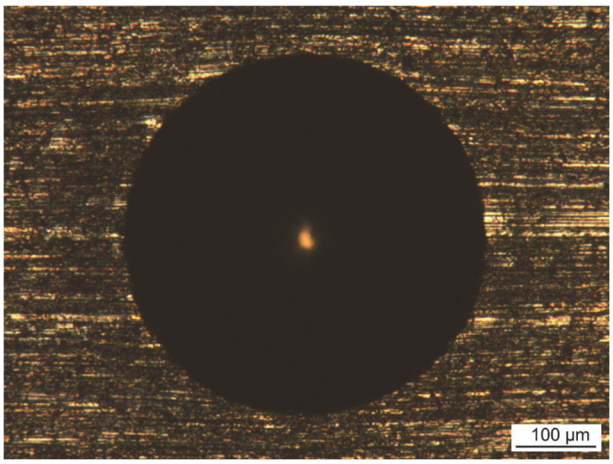

Figure 5: Imprint on a coated sample after Rockwell-C adhesion test.

Rolling contact fatigue behavior

Fig. 6 shows a representative profile of the rolling track (RT) of the coated specimens. This profile does not show material build up at the edges of the RT. Furthermore, since the RT width is several orders of magnitude greater than its depth, it is considered that the deformation suffered by the contact area is negligible and, therefore, that the tests were valid.

Failure in uncoated AISI 440C samples were characterized by the typical concentrated damage in the form of spalls, as shown in Fig. 7. As can be seen, the spall size is comparable to the RT width. The rolling direction (RD) is indicated in the micrograph. In addition, a polishing effect of the RT in the uncoated specimens can be observed, as shown in Fig. 8. This confirms the interaction between the surface asperities of the contact bodies, as predicted by the λ values calculated.

On the other hand, all failures in coated samples were characterized by partial coating delamination, with no substrate spalling, as shown in Fig. 9. This failure mode is consistent with one of those commonly observed in coated samples [15]. It is worth mentioning that coating delamination is a damage in the coating itself and not in the substrate. However, it would not be admissible in most mechanical applications because of oil contamination and other possible consequences.

The EDS analysis performed inside a delaminated area and outside the RT of a coated specimen is shown in Fig. 10. It can be noted that the EDS spectrum taken inside the delaminated area revealed the presence of Fe, Cr and C peaks, the main constituents of AISI 440C, while the Ti content, in contrast to what was revealed outside the RT was practically negligible. In this case, some substrate polishing can also be seen due to asperities contact after coating delamination.

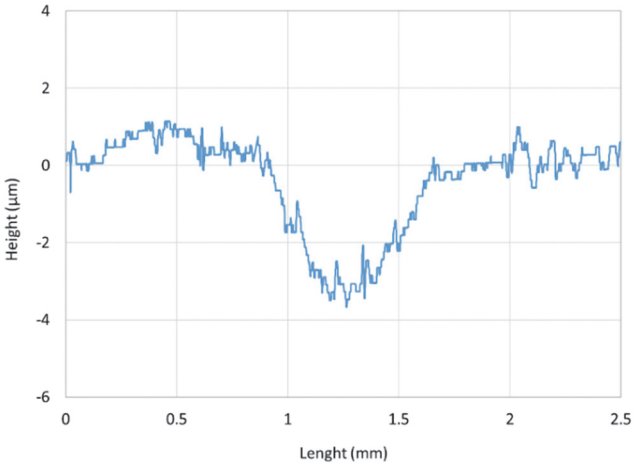

Figure 6: Rolling track profile of a coated sample.

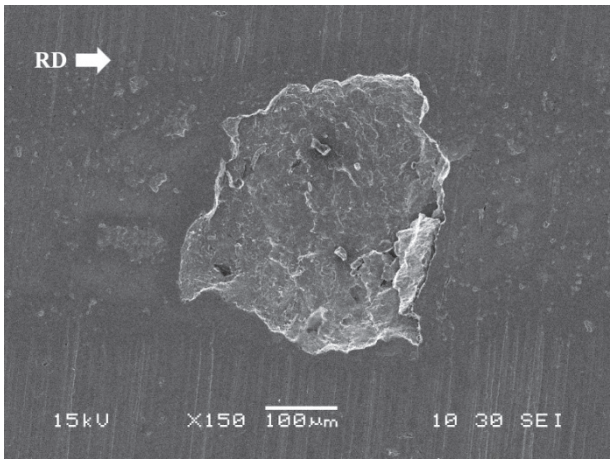

Figure 7: RCF failure in an uncoated sample.

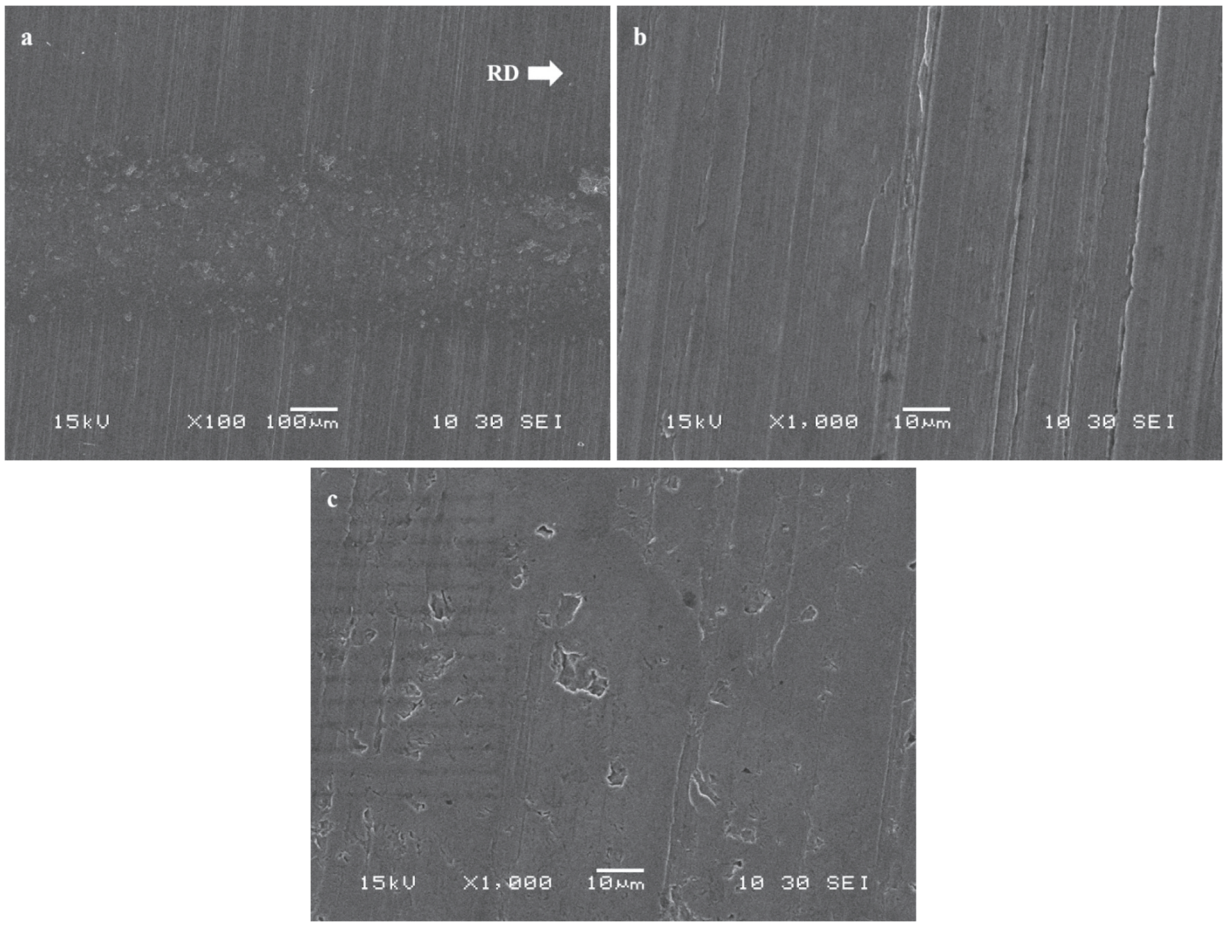

Figure 8: SEM images of an uncoated sample. a) portion of the rolling track, b) a detailed image outside the rolling track, c) a detailed image inside the rolling track.

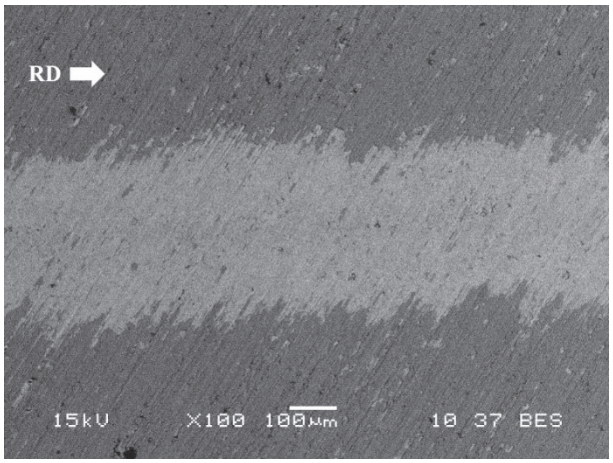

Figure 9: RCF failure in a coated sample.

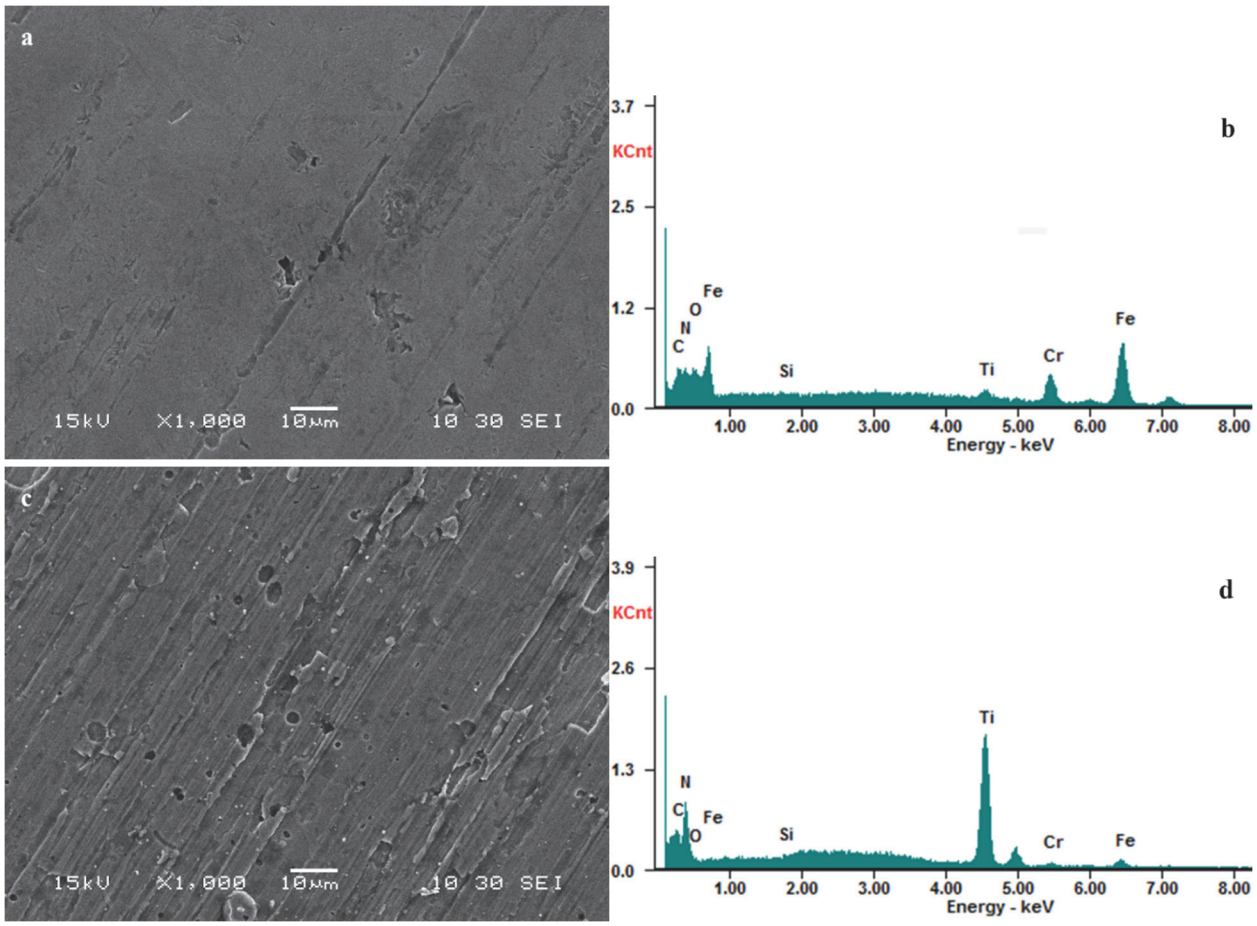

Figure 10: SEM images and EDS analysis of a coated sample. a) and b) inside the rolling track, c) and d) outside the rolling track.

The relation between the failure probability and the number of loading cycles for the uncoated and coated samples are shown in the Weibull plot of Fig. 11. The results of the Weibull analysis are summarized in Tab. 3, reflecting the characteristic life or scale parameter (η), the shape parameter (β) and the coefficient of determination (R^2). The resulting characteristic life of the coated samples is more than four times higher than that of the uncoated ones.

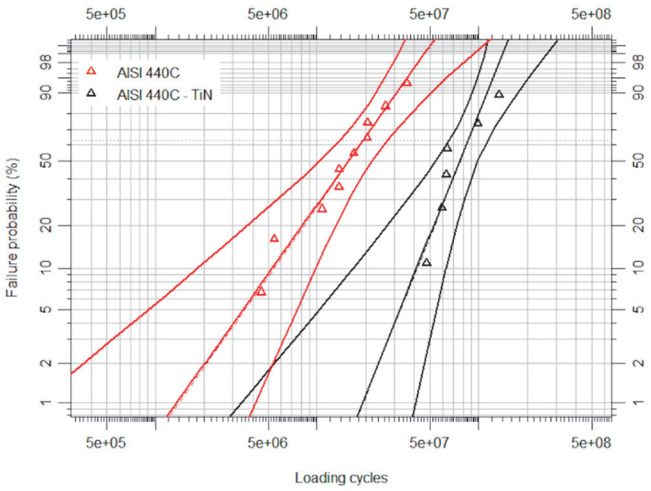

Figure 11: Weibull plot for the uncoated and coated samples.

Sample	η(cyclesx10⁶)	β	R^2
AISI 440C	19.23	1.73	0.97
AISI 440C-TiN	85.79	3.06	0.83

Table 3: Weibull parameters for the uncoated and coated samples.

Tab. 4 compares the L10 and L50 estimates for the uncoated and coated samples and the corresponding confidence intervals. As was observed with characteristic life, the L10 and L50 estimates of the coated samples are higher than those of the uncoated ones. In addition, the estimated confidence intervals indicate that the application of TiN coatings by PBII&D produces a significant increase of the RCF endurance of AISI 440C. This behavior is consistent with previous studies conducted on austempered ductile iron substrates coated by PBII&D [20]. Similar results have also been reported on high hardness steels coated by PBII&D [23-25], but the absence of relevant experimental data in those works, such as tempering temperature, deposition temperature, RCF lubrication regime and/or RCF confidence intervals, does not allow conclusive statements to be drawn or comparisons to be made. The good performance of PBII&D coatings against RCF, as compared to other PVD coatings [20], suggests that under a boundary lubrication regime, the gradient interface is capable to lengthen the nucleation stage of the substrate failure process. The non-hardness reduction of AISI 440C substrates produced by the room temperature deposition also contributes to the good RCF performance of the PBII&D coatings.

Sample	L10(cycle x10⁶)		L50 (cycles x10⁶)	
	Estimate	Confidence interval	Estimate	Confidence interval
AISI 440C	5.25	1.88-9.69	15.57	10.29-21.95
AISI 440C-TiN	41.17	17.06-63.01	76.12	54.45-98.78

Table 4: L10 and L50 estimates for the uncoated and coated samples.

CONCLUSIONS

This work studied the microstructural evolution, surface characteristics and RFC behavior of high hardness AISI 440C samples coated with a TiN film synthesized by PBII&D at room temperature. Based on the results obtained, the following conclusions can be drawn:

- The microstructure of the substrates, formed by martensite with very fine needles, retained austenite and a network of dispersed carbides, remained unchanged after the deposition process. In addition, the hardness of the substrates was

maintained between 59 HRC and 60 HRC before and after deposition. The grinding operations produced fairly symmetrical profiles (Rsk ≈ 0) with low Ra.

- The application of the coatings produced an increase in Ra and a change in the skewness of the profiles (Rsk > 0). The adhesion of the coatings was of good quality, proper of PVD coatings deposited at temperatures above 300 °C. This good adhesion can be ascribed to the mixing zone formed by the PBII&D process at the substrate/coating interface.
- RCF test generated typical fatigue spalls in the uncoated samples. In coated samples partial delamination of the coating occurred along the rolling track. Taking the partial delamination of the coating as a failure criterion, it was found that the RCF life of the coated samples was higher than that of the uncoated ones.
- The good performance of PBII&D coatings against RCF suggests that under a boundary lubrication regime, the gradient interface is capable of lengthening the nucleation stage of the failure process. The non-hardness reduction of AISI 440C substrates also contributes to the good RCF performance of the coatings.

ACKNOWLEDGEMENTS

The authors wish to thank the company "Orengia y Conforti ICSA" for the donation of the AISI 440C bars. The experimental equipment support granted by INTEMA-CONICET, the INFIP and the National University of Mar del Plata is also gratefully acknowledged.

REFERENCES

[1] Sadeghi, F., Jalalahmadi, B., Slack, T. S., Raje, N. and Arakere, N. K. (2009) A Review of Rolling Contact Fatigue, J. Tribol., 131(4). DOI: 10.1115/1.3209132.

[2] Bhalerao, V. Y. and Lakade, S. S. (2022). Comprehensive review on improvement in surface properties of bearing steel, Materials Today: Proceedings, 55, pp. 441-446. DOI:10.1016/j.matpr.2022.01.481.

[3] Krella, A. (2020). Resistance of PVD Coatings to Erosive and Wear Processes: A Review, Coatings, 10(10), pp. 921. DOI: 10.3390/coatings10100921.

[4] Çomaklı, O. (2021). Improved structural, mechanical, corrosion and tribocorrosion properties of Ti45Nb alloys by TiN, TiAlN monolayers and TiAlN/TiN multilayer ceramic films, Ceram. Int., 47(3), pp. 4149-4156. DOI: 10.1016/j.ceramint.2020.09.292.

[5] Vengesa, Y., Fattah-alhosseini, A., Elmkhah, H., Imantalab, O. and Keshavarz, M. K. (2023). Investigation of corrosion and tribological characteristics of annealed CrN/CrAlN coatings deposited by CAE-PVD, Ceram. Int., 49(2), pp. 3016-3029. DOI: 10.1016/j.ceramint.2022.09.286.

[6] Stewart, S. and Ahmed, R. (2002). Rolling contact fatigue of surface coatings - a review, Wear, 253(11-12), pp. 1132-1144. DOI: 10.1016/S0043-1648(02)00234-X.

[7] Ostadi, A., Hosseini, S. H. and Fordoei, M. E. (2020). The effect of temperature and roughness of the substrate surface on the microstructure and adhesion strength of EB-PVD ZrO2-%8wtY2O3 coating, Ceram. Int., 46(2), pp. 2287-2293. DOI: 10.1016/j.ceramint.2019.09.217.

[8] Sproul, W. D., Graham, M. E., Wong, M.-S. and Rudnik, P. J. (1993). Reactive unbalanced magnetron sputtering of the nitrides of Ti, Zr, Hf, Cr, Mo, Ti-Al, Ti-Zr and Ti-Al-V, Surf. Coat. Technol., 61(1), pp. 139-143. DOI: 10.1016/0257-8972(93)90216-B.

[9] Thom, R., Moore, L., Sproul, W. D. and Peter Chang, T. (1993). Rolling contact fatigue tests of reactively sputtered nitride coatings of Ti, Zr, Hf, Cr, Mo, Ti-Al, Ti-Zr and Ti-Al-V on 440C stainless steel substrates, Surf. Coat. Technol., 62(1–3), pp. 423-427. DOI: 10.1016/0257-8972(93)90278-V.

[10] Naebe, M. and Shirvanimoghaddam, K. (2016). Functionally graded materials: A review of fabrication and properties, Appl. Mater. Today, 5, pp. 223-245. DOI: 10.1016/j.apmt.2016.10.001.

[11] Inoue, S., Ucihda, H., Takeshita, K., Koterazawa, K. and Howson, R. P. (1995). Preparation of compositionally gradient Ti-TiN films by r.f. reactive sputtering, Thin Solid Films, 261(1–2), pp. 115-119. DOI: 10.1016/S0040-6090(95)06527-X.

[12] PalDey, S. and Deevi, S. C. (2003). Properties of single layer and gradient (Ti,Al)N coatings, Mater. Sci. Eng., A, 361(1–2), pp. 1-8. DOI: 10.1016/S0921-5093(03)00473-8.

[13] Pelletier, J. and Anders, A. (2005). Plasma-Based Ion Implantation and Deposition: A Review of Physics, Technology and Applications, IEEE Transactions on Plasma Science, 33, pp. 1944-1959. DOI: 10.1109/TPS.2005.860079.

[14] Heinke, W., Leyland, A., Matthews, A., Berg, G., Friedrich, C. and Broszeit, E. (1995). Evaluation of PVD nitride coatings, using impact, scratch and Rockwell–C adhesion tests, Thin Solid Films, 270(1-2), pp. 431-438. DOI: 10.1016/0040-6090(95)06934-8.
[15] Holmberg, K. and Matthews, A. (2009). Coatings Tribology: Properties, Mechanisms, Techniques and Applications in Surface Engineering, Elsevier, Oxford, UK. ISBN: 9780444527509
[16] Abernethy, R. B. (2000). The New Weibull Handbook, R.B. Abernethy, Florida, USA. ISBN: 0-9653062-1-6.
[17] McCool, J. I., (2012). Using the Weibull Distribution: Reliability, Modeling and Inference, Wiley, New Yersey, USA. ISBN: 978-1-118-21798-6.
[18] Jalaja, K., Manwatkar, S. K., Anand, P., Rejith, R. and Narayana Murty, S. V. S. (2021). Metallurgical analysis of surface distress on balls during the operation of AISI 440C ball bearings for satellite applications, Engineering Failure Analysis, 124, pp. 105376. DOI: 10.1016/j.engfailanal.2021.105376.
[19] Shiao, M.-H. and Shieu, F.-S. (2001). A formation mechanism for the macroparticles in arc ion-plated TiN films, Thin Solid Films, 386(1), pp. 27-31. DOI:10.1016/S0040-6090(00)01918-0.
[20] Quintana, J. P., Massone, J. M., Márquez, A. B. and Colombo, D. A. (2019). Rolling contact fatigue behavior of TiN based coatings deposited on ADI by cathodic arc deposition and plasma based ion implantation and deposition, Thin Solid Films, 671, pp. 95-102. DOI: 10.1016/j.tsf.2018.12.014.
[21] Vaca, L. S., Quintana, J. P., Vega, D., Márquez, A. and Brühl, S. P. (2021). Tribological and corrosion Behavior of Duplex Coated AISI 316L using plasma based ion implantation and deposition, Materials Today Communications, 26, pp. 101892. DOI: 10.1016/j.mtcomm.2020.101892.
[22] Colombo, D. A., Echeverría, M. D., Moncada, O. J. and Massone, J. M. (2012). PVD TiN and CrN coated austempered ductile iron: analysis of processing parameters influence on coating characteristics and substrate microstructure, ISIJ Int., 52(1), pp. 121-126. DOI: 10.2355/isijinternational.52.121.
[23] Hongxi, L., Yehua, J., Rong, Z. and Baoyin, T. (2012). Wear behaviour and rolling contact fatigue life of Ti/TiN/DLC multilayer films fabricated on bearing steel by PIIID, Vacuum, 86(7), pp. 848-853. DOI: 10.1016/j.vacuum.2011.02.015.
[24] Liu, H. X., Jiang, Y. H., Zhou, R., Li, Z. L. and Tang, B. Y. (2008). Investigating the Mechanical Property and Rolling Contact Fatigue Life of Diamond-Like Carbon Films on Bearing Steel, Materials Science Forum, 575-578, pp. 990-995. DOI: 10.4028/www.scientific.net/MSF.575-578.990.
[25] Liu, H.-x., Wang, X.-f., Wang, L.-p. and Tang, B.-y. (2007). Rolling contact fatigue and mechanical properties of titanium carbide film synthesized on bearing steel surface, Surf. Coat. Technol., 201(15), pp. 6606-6610. DOI: 10.1016/j.surfcoat.2006.09.105.